MRI and pathology correlations in the medulla in sudden unexpected death in epilepsy (SUDEP): a postmortem study

S. Patodia*†, M. Tachrount‡§, A. Somani*†, I. Scheffer¶, T. Yousry‡, X. Golay‡, S. M. Sisodiya†** and M. Thom*† (iD)

*Department of Neuropathology, UCL Queen Square Institute of Neurology, London, UK, †Clinical and Experimental Epilepsy, UCL Queen Square Institute of Neurology, London, UK, ‡Neuroradiology Academic Unit,Brain Repair and Rehabilitation,UCL Queen Square Institute of Neurology, London, UK, §FMRIB, Nuffield Department of Clinical Neurosciences, Wellcome Centre for Integrative Neuroimaging, University of Oxford, Oxford, UK, ¶Department of Medicine (Neurology), Epilepsy Research Centre, University of Melbourne, Melbourne, VIC, Australia and **Chalfont Centre for Epilepsy, Chalfont St Peter, UK*

S. Patodia, M. Tachrount, A. Somani, I. Scheffer, T. Yousry, X. Golay, S. Sisodiya and M. Thom (2020) *Neuropathology and Applied Neurobiology* **MRI and pathology correlations in the medulla in sudden unexpected death in epilepsy (SUDEP): a postmortem study**

Aims: Sudden unexpected death in epilepsy (SUDEP) likely arises as a result of autonomic dysfunction around the time of a seizure. *In vivo* MRI studies report volume reduction in the medulla and other brainstem autonomic regions. Our aim, in a pathology series, is to correlate regional quantitative features on 9.4T MRI with pathology measures in medullary regions. **Methods**: Forty-seven medullae from 18 SUDEP, 18 nonepilepsy controls and 11 epilepsy controls were studied. In 16 cases, representing all three groups, *ex vivo* 9.4T MRI of the brainstem was carried out. Five regions of interest (ROI) were delineated, including the reticular formation zone (RtZ), and actual and relative volumes (RV), as well as T1, T2, T2* and magnetization transfer ratio (MTR) measurements were evaluated on MRI. On serial sections, actual and RV estimates using Cavalieri stereological method and immunolabelling indices for myelin basic protein, synaptophysin and Microtubule associated protein 2 (MAP2) were carried out in similar ROI. **Results**: Lower relative RtZ volumes in the rostral medulla but higher actual volumes in the caudal medulla were observed in SUDEP ($P < 0.05$). No differences between groups for T1, T2, T2* and MTR values in any region was seen but a positive correlation between T1 values and MAP2 labelling index in RtZ ($P < 0.05$). Significantly lower MAP2 LI were noted in the rostral medulla RtZ in epilepsy cases ($P < 0.05$). **Conclusions**: Rostro-caudal alterations of medullary volume in SUDEP localize with regions containing respiratory regulatory nuclei. They may represent seizure-related alterations, relevant to the pathophysiology of SUDEP.

Keywords: 9.4T MRI, medullary raphe, medulla, SUDEP, ventrolateral medulla

---

Introduction

Sudden unexpected death in epilepsy (SUDEP) is the leading cause of death in young adults with intractable epilepsy and may have many causes [1]. Recent clinical, neuroimaging and experimental research provides converging evidence for a central failure of autonomic regulation of cardiovascular and

respiratory function in SUDEP [1,2]. Brainstem autonomic dysfunction, including vital cardiorespiratory regulation in the postictal period, may represent a final common pathway.

The primary risk factor, based on meta-analysis of SUDEP series, is poor control of generalized tonic-clonic seizures (GS) [3,4]. Following GS, irregular, shallow breathing [5] and ictal central apnoea with hypercapnia and hypoxaemia are not infrequent [6-8]. SUDEP often occurs nocturnally or during sleep [9] and convergence of impaired brainstem arousal systems interacting with inadequate respiratory drive during seizures may also be relevant. In experimental models of SUDEP, spreading depolarizations to the dorsal medulla following seizures have also been shown to mediate cardio-respiratory arrest [10]. In structural MRI studies, volume loss in the medulla in SUDEP has been shown in some but not all studies [11-13].

Central control of respiration is regulated by interconnected medullary nuclear groups forming the ventral respiratory column [14]. One such nucleus is the pre-Bötzinger complex (pre-BötC), an essential generator of inspiratory rhythm [15]. The pre-BötC forms an ill-defined region in the reticular zone (RtZ) of the medulla, more specifically in the ventro-lateral medulla (VLM) comprising mixed neuronal types with high levels of somatostatin and neurokinin 1 receptor (NK1R) expression [16,17]. It is modulated by other brainstem nuclear groups, including the serotonergic neurones of the medullaryh raphe (MR) [18]. In previous studies of the medulla in SUDEP, we have shown regional alterations in specific neuronal and glial subsets including serotonergic and neuropeptidergic neurones, potentially relevant to medullary dysfunction [19,20]. Whether subtle cellular alterations in medulla contribute to regional volume changes or alteration of MRI signal is unknown.

In this postmortem study, we aimed to study volume and signal changes in high resolution 9.4T MRI of postmortem brainstem samples from SUDEP cases compared to control groups, including in the RtZ and VLM regions. We also explored pathological correlations for any volume or signal changes using quantitative immunohistochemistry for myelin, neuronal somato-dendritic and synaptic markers in these regions.

Methods

Case selection

Brainstems from 29 epilepsy cases were included in this study (Table 1). The study has ethical approval with appropriate consent for research for all cases included in the study. Tissue from all postmortem cases was retained with era-appropriate consent collected through the Epilepsy Society Brain and Tissue Bank (ESBTB) at UCL and *Brain UK* via the pathology department at Derriford Hospital, Plymouth, UK. The epilepsy cases included Dravet syndrome cases obtained from the University of Melbourne, Australia (as previously reported [21]). The cause of death for epilepsy cases was categorized as SUDEP in 18 cases or a non-SUDEP death in 11 cases (Epilepsy control group, EPC) according to current criteria [22]. 18 nonepilepsy controls (NEC) with no history of epilepsy were included, obtained through ESBTB and the MRC Brain and tissue Bank, Edinburgh. The clinical and neuropathology records, including epilepsy history, circumstances of death and main neuropathology findings are detailed in Table S1. Of note, both EPC and SUDEP groups included cases with recent onset of epilepsy (in the last year 2 years of life).

Brainstem 9.4T MRI

In 16 cases (6 SUDEP, 3 EPC, 7 NEC), MRI imaging of whole or hemi-brainstems, fixed in 10% formalin for at least 1 week, was carried out (Figure 1A,B). In six cases (representing cases from all patient groups) in order to adequately fit the sample in the MRI radio-frequency coil without distortion, just hemi-brainstems were scanned. In those cases, the sagittal plane of the section was taken to one side of the midline to ensure inclusion of central raphe nuclei (Figure S1A,B). The samples were scanned on a 9.4T MRI scanner (Agilent Technologies, Santa Clara, CA, USA) using a volume coil with a diameter of 33 mm (Rapid Biomedical GmbH, Rimpar, Germany). After manual global shimming and acquiring fast localization images, a T2-weighted (T2W) scan in addition to quantitative T1, T2, T2* and magnetization transfer ratio (MTR) mapping sequences were applied as in our previous study [23]. To get an in-plane spatial resolution of

Table 1. Summary of clinical details for the four groups studied (detailed case information is provided in Table S1)

Group N = total number in study [Cases with MRI]	Male:Female [Cases with MRI]	Mean age onset of epilepsy/ (range in years) [Cases with MRI]	Mean age of death (range in years) [Cases with MRI]	Mean brain weights (fresh) (range) [Cases with MRI]	PMI/fixation times Mean (range in days) [Cases with MRI]	Mean mid obex level (range in mm)
Sudden unexpected death in epilepsy N = 18 [6]	12:6 [5:1]	10.8 (1–39) [11.9 (1–26)]	34 (1–53) [41 (1–47)]	1382 g (1078–1668)g [1449 (1220–1668)]	3 (1–7)/35 (5–98) [3.6 (1–5)/ 32.6 (16–51)]	6.7 (3.5–10) [6.7 (4–9)]
Epilepsy controls N = 11 [3]	7:4 [2:1]	17 (1–84) [48 (12–84)]	60 (5–86) [41 (27–53)]	1292 g (1125–1490)g [1350 (1223–1490)]	2.4 (1–5)/44 (1–90) [2.6 (1–5)/28 (11–49)]	6.5 (3–10.5) [6.1 (3–8.5)]
Non-epilepsy controls N = 18 [7]	11:7 [2: 5]	–	41 (23–80) [46 (25–80)]	1426 g (1223–1650)g [1348 (1223–1602)]	3.2 (1–6)/25.5 (7–94) [4 (2–6)/42.8 (24–94)]	6.6 (3–11.5) 5.5 (3–11)]
Significant differences between groups	$P = 0.69$ [0.15]	$P = 0.6$ [0.35]	**$P = 0.005$** [0.95]	$P = 0.16$ [0.26]	$P = 0.47/P = 0.24$ [0.51/0.68]	$P = 0.73$ [0.46]

Differences between groups with nonparametric tests; significant differences shown in bold.
PMI, postmortem interval (time between death and postmortem examination); Fixation time, time brain fixed in formalin prior to processing.

100×100 μm^2 and a slice thickness of 400 μm for all the samples, the field of view, the size of the acquisition matrix and the number of slices were adjusted according to the size of each sample. The FOVs used had a range of 34×34 mm^2 to 30×24 mm^2 and the number of slices ranged between 80 and 120. A multislice spin echo (SEMS) scan with TE/TR = 35/ 8000 ms was applied to obtain T2W images. The acquisition time (TA) was about 8 h. For the T1 mapping, a multi-TR saturation recovery approach was applied using a SEMS sequence (TE = 12 ms and TRs = 0.35/0.5/0.85/1.5/3/9.5 s). For short TRs, several slice packages with a fewer number of slices and different offsets were acquired separately and then combined to obtain a full coverage of the sample. The number of averages was adapted for each TR to obtain a good signal-to-noise ratio. The number of slices was 10 for TRs = 350/500 ms (NA = 8) and 40 for TRs = 850/1500 ms (NA = 3). For the long TRs (3 s and 9.5 s), all the slices were acquired in a single scan. The NAs were 2 and 1 for TR of 3 s and 9.5 s respectively. The acquisition time of all the saturation recovery scans depended on the number of slices and it was about 7.5 h for 80 slices. For the T2 mapping, a multi-echo SEMS sequence with a TR = 8 s and TEs = 15/ 25/35/60 ms was used (TA = 9 h). A multislice multigradient echo sequence with TR = 5 s, TE = 5.5/ 13.5/21.5 ms and flip angle (FA) of 90° was applied for the T2* mapping (TA = 6 h). For the MTR mapping, a multislice gradient echo sequence with TE/ TR = 10/4200 ms and FA = 40° (TA = 7.5 h) was applied. The magnetization transfer RF pulse was applied with a FA of 500° and frequency offsets of 6 kHz (MT weighted) and 100 kHz (control). The total scanning time for the entire protocol including the adjustments was approximately 39 h. MRI Relaxation times T1, T2, T2* and MTR maps were obtained by processing the data using both an in-house developed script running under Matlab (Mathworks, Natick, Massachusetts, USA) and ImageJ (National Institutes of Health, Bethesda, MD, USA; http://imagej.nih.gov/ij/in dex.html) and the mean relaxation times for T1, T2, T2* were calculated for each case in different medulla regions to evaluate grey and white matter and MTR values for myelin integrity (detailed below).

Cavalieri method for medulla volume estimations

Following the MRI scanning, medulla blocks were cut at 5 mm intervals from obex 0 mm (the caudal recess of the fourth ventricle) in an axial plane to the upper brainstem, using a cutting guide. For all 47 cases, a
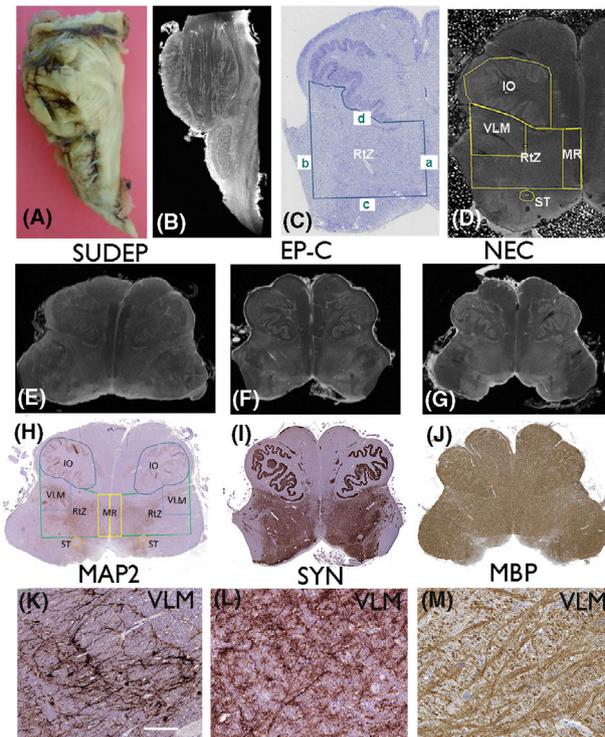
Figure 1. 9.4T MRI and pathology quantitative analysis of medullary regions. (**A**) Whole fixed brainstem from sudden unexpected death in epilepsy (SUDEP) (case 1) and (**B**) sagittal section following 9.4T MRI. (**C**) Cresyl violet stained section (obex 10) showing the boundaries of the reticular zone (RtZ) region of interest (ROI) used for the Cavalieri volume estimations defined as follows: (a) medial boundary (midline of the brainstem), (b) lateral boundary (line parallel to the midline touching the lateral end of the inferior olive (IO), (c) dorsal boundary (line perpendicular to the midline at the ventral end of the solitary tract) and (d) ventral boundary (line perpendicular to midline, at medial end of IO, and following the contour of the IO to meet the lateral boundary). (**D**) Axial MRI section (obex 10) with ROI indicated: RtZ, using the same boundaries as described for the Cavalieri volume estimation; VLM (ventrolateral medulla), representing the geometric ventrolateral quadrant within the RtZ as previously described [20]; MR (median racphe), using a line parallel to midline drawn from the halfway point between the medial end of the tip of the IO and the midline, IO, drawing around nucleus and hilus freehand, excluding accessory nuclei; ST (solitary tract), drawing around the contours of the solitary tract. (**E**) T2 weighted images of axial section from SUDEP medulla (case 13, mid-obex level +5 mm), (**F**) Epilepsy control case (EP-C case 40, mid obex level +8.5 mm) and (**G**) Nonepilepsy control (NEC, case 44, mid obex level +7 mm). (**H**) MAP2 stained section of SUDEP case shown in **E** with ROI for quantitative analysis indicated. (**I**) Synaptophysin immunostained section of EP-C case shown in **F**. (**J**) Myelin basic protein (MBP) of NEC case shown in **G**. (**K**) MAP2 labelling of neurones and dendritic process in the VLM region (case in **H**). (**L**) Synaptophysin labelling in the VLM showing more diffuse granular labelling decorating axons and cell bodies. (**M**) MBP in the VLM showing crossing myelinated bundles around neurones. Bar shown approximates to 1 cm in **A**, **B**, 2 mm in **C**, **D**, 1 mm in **E–J** and 200 μ in **K–M**.

single block from the medulla blocks was selected, aiming to include obex level 6 to 12 mm where available, as the putative level of the human preBötC [24].

Serial sections through each block were cut at 20 μm thickness using the Tissue-Tek AutoSection automated microtome (Sakura Finetek, Torrance, CA, U.S.A. Inc) obtaining 150–200 sections per case. Every 10th section (200 μm steps) was stained with cresyl-violet (CV) as previously described [20]. The obex levels of each section were determined independently by two observers (MT, SP) according to the atlas of Paxinos [25]. Ten CV sections at 200 um equidistance (equivalent to 2000 μm) were selected for volume estimation, nearest to the preBötC region in the VLM. Using the Cavalieri method (StereoInvestigator Software; MBF Biosciences, Williston, VT) the volume of RtZ was measured in each case, in addition to two control regions of interest (ROI) the 12th cranial nerve nuclei (12 CNN) and inferior olive nuclei (IO) as comparisons. For whole brainstem sections, both left and right sides were analysed and averaged. The boundaries of RtZ ROI were defined as follows: medial boundary (midline of the brainstem), lateral boundary (line parallel to the midline touching the lateral end of the IO, dorsal boundary (line perpendicular to the midline at the ventral end of the solitary tract) and ventral boundary (line perpendicular to midline, at medial end of IO, and following the contour of the IO to meet the lateral boundary) (Figure 1**C**). The RtZ ROI therefore captured all nuclei of the reticular formation (intermediate, lateral, ventral, dorsal and gigantocellular nuclei) and the ventral medullary respiratory column as well as the nucleus ambiguus (NA) and MR nucleus obscurus [25]. The contours of the IO and 12 CNN were manually outlined and selected as control regions as they could be easily anatomically identified on CV sections. The actual volume (AV) of the RtZ as well as a relative volume (RV) RtZ volume/total volume of all ROI was calculated. The RV was calculated to factor for case to case differences, differential shrinkage from fixation and processing as well as tilts in the axial plane of cut between cases. The coefficient of error was 0.05 or less in all volume measurements for each case.

MRI and alignment and quantitation

The MRI image slices were manually co-aligned with the 10 CV sections selected for the Cavalieri volume estimation (Figure S1A,B). Distinct anatomical

landmarks (folds in the olivary nuclei, vascular structures, contours of the ventricles etc.) were used independently by two observers (SP, MT) to match the MRI slices that corresponded to the range of serial CV sections selected for the Cavalieri volume method. The mean number of MRI slices per case was 8 (range 7–10). Using the freehand selection drawing tool on Image J, the following ROIs were drawn (Figure 1D): *RtZ* (using the same boundaries as described for the Cavalieri volume estimation), *VLM* (representing the ventrolateral quadrant within the RtZ using boundaries as previously described [20]), *MR* (using a line parallel to midline drawn from the halfway point between the medial end of the tip of the IO and the midline), *IO* (drawing around nucleus and hilus freehand, excluding accessory nuclei), *ST* (drawing around the contours of the solitary tract). The mean quantitative MRI (qMRI) values for T1, T2, T2*, and MTR values and volume estimate were obtained for each ROI across 10 levels. The RV of the VLM to the total volume of medullary regions for each case was obtained.

Immunohistochemistry and quantification

Further sections from the mid-obex region of each case were immunolabelled for myelin basic protein [MBP, clone SMI94 (Sternberger, Lutherville, MD, USA); 1:2000 dilution] as a measure of myelin integrity, MAP2 [clone HM-2 (Sigma M4403, Welwyn Garden City, UK); 1:5000 dilution] as a neuronal soma/dendritic marker and synaptophysin [clone DAK-SYNAP (DAKO, Stockport, England); 1:100 dilution] for grey matter, on Leica Bond max automated IHC stainer. The UCLH + enhancer protocol was applied which included pretreatment (ENZ1 for 10 min for MBP, ER1 for 30 min for MAP2, and ER2 for 20 min for synaptophysin), followed by 15 min incubation with primary antibody, 8 min each with postprimary and polymer, 10 min with DAB, 5 min with DAB enhancer, and 5 min with haematoxylin. The slides were washed with Bond-wash solution between all steps. Slides were scanned with a Leica SCN400F digital slide scanner (Leica Microsystems, Wetzlar, Germany) at 40× magnification. Analysis of immunostained sections was carried out with Definiens Tissue Studio 3.6 (Definiens AG, Munich, Germany). Five ROIs were outlined using co-ordinates as detailed in the MRI study (Figure 1H) and including both sides where available. Any defects in the section, for example small tissue folds or staining artefacts, were carefully outlined and excluded from the analysis. Intensity thresholds for detection of each marker were developed through training a range on representative sections and areas, then applied to all cases and the mean labelling index (LI) for each ROI calculated averaged for both sides.

Statistical analysis and graphical representation

Statistical analysis was carried out using SPSS (IBM version 21, IBM Corp., Armonk, NY, USA) and (Graph-Pad Prism software, San Diego, CA, USA) was used for the graphical representation of the data. Nonparametric correlation (Kendal's τ) and Mann–Whitney tests were used for comparison between groups, with clinical and postmortem factors. Uncorrected values of $P < 0.05$ were taken as significant with corrections for multiple comparisons. Multiple regression analysis was used to evaluate effects of other variables (postmortem delay, obex level) on measurements between the cause of death groups.

Results

Volume estimations with 9.4T MRI and Cavalieri method

There were no significant differences in MRI volume estimations (actual and relative) between the cause of death groups (SUDEP, EP-C, NEC) (Table 2); when comparing all epilepsy cases to NEC, significantly higher AVs were noted in the IO ROI in epilepsy ($P < 0.05$). Cavalieri method volume estimates on the entire series, including cases with MRI, also showed no difference in actual or RV estimates of the RtZ between the three cause of death groups (Table 2). There was also no difference in mean RtZ volume when all epilepsy cases were compared to NEC. A positive correlation with MRI and Cavalieri volume estimates of the RtZ was noted for all 16 cases ($P < 0.05$) but with lower volume estimates using the Cavalieri method (Figure S1C).

Quantitative MRI, immunohistochemistry and correlations

qMRI values showed no differences for T1, T2, T2* and MTR values between the three cause of death groups for any ROI. There were also no differences

Table 2. Quantitative MRI values for the regions of interest and volume estimates

Mean (SD)	SUDEP Mean (SD)	EPC Mean (SD)	NEC Mean (SD)
MRI T1 values			
RtZ	0.99 (0.07)	1.11 (0.26)	1.05 (0.19)
VLM	1.02 (0.09)	1.13 (0.27)	1.06 (0.18)
IO	1.04 (0.07)	1.19 (0.27)	1.11 (0.21)
ST	1.03 (0.08)	1.18 (0.29)	1.13 (0.24)
MR	1.00 (0.07)	1.09 (0.26)	0.86 (0.38)
MRI T2 values			
RtZ	0.024 (0.003)	0.027 (0.005)	0.023 (0.003)
VLM	0.025 (0.003)	0.028 (0.005)	0.024 (0.003)
IO	0.024 (0.003)	0.027 (0.006)	0.023 (0.003)
ST	0.025 (0.003)	0.029 (0.006)	0.025 (0.004)
MR	0.024 (0.003)	0.026 (0.005)	0.024 (0.003)
MRI T2* values			
RtZ	0.015 (0.003)	0.018 (0.004)	0.017 (0.003)
VLM	0.015 (0.003)	0.018 (0.004)	0.017 (0.003)
IO	0.015 (0.003)	0.018 (0.004)	0.017 (0.003)
ST	0.018 (0.001)	0.020 (0.004)	0.018 (0.004)
MR	0.013 (0.003)	0.017 (0.004)	0.016 (0.003)
MRI MTR values			
RtZ	6168 (1634)	1204[†]	6799 (2569)
VLM	6270 (1680)	1230	6770 (2625)
IO	6548 (1676)	1261	6940. (2688)
ST	7235 (1814)	1396	7132 (2021)
MR	5516 (1528)	1080	6398 (2429)
MRI volumes (10^2 mm^3)			
RtZ	1.91 (9.2)	1.69 (0.113)	1.806 (0.18)
VLM	0.633 (0.039)	0.544 (0.084)	0.567 (0.124)
IO	1.27 (0.187)	1.154 (0.149)	1.046 (0.175)
ST	0.035 (0.007)	0.023 (0.0008)	0.026 (0.009)
MR	0.307 (0.064)	0.273 (0.0395)	0.315 (0.073)
VLM (relative)	0.18 (0.01)	0.17 (0.02)	0.17 (0.02)
Cavalieri volume (mm^3)			
RtZ (actual)	30.74 (6.4)	27.36 (3.9)	31.52 (7.3)
RtZ relative	0.739 (0.03)	0.72 (0.02)	0.74 (0.02)

RtZ, reticular zone; VLM, ventrolateral medulla; IO, inferior olive; ST, solitary tract; MR, median racphe; MTR, magnetization transfer ratio.
[†]MTR values were available from only one of the epilepsy control cases.

when all epilepsy cases were compared to NEC (Table 2). MAP2 labelling highlighted neurones and dendritic processes in the RtZ, VLM and other ROI (Figure 1H,K). There was a positive correlation between T1 values and MAP2 LI in RtZ ($P < 0.05$) (Figure 2A) and VLM ROI ($P < 0.05$) (Figure 2B) for all 16 cases. Synaptophysin showed more diffuse granular labelling in grey matter regions (Figure 1I,L) and variable intensity between cases; there was no correlation between synaptophysin labelling and qMRI measures. SMI94/MBP labelled dense myelinated bundles in all ROI (Figure 1J,M); there was negative correlation between SMI94/MBP LI and T2* in the ST but a positive correlation with MTR ($P < 0.05$) in the ST (Figure 2C) and T2 in the IO region.

In the 47 cases studied, SMI94/MBP LI was significantly lower in epilepsy groups than in NEC in the VLM ($P < 0.01$), RtZ ($P < 0.05$) but there were no significant differences between SUDEP and EPC groups (Figure 2D). MAP2 LI was significantly lower in the epilepsy groups than NEC for all ROI ($P < 0.05$ to $P < 0.001$), but there were no significant differences between EPC and SUDEP groups (Figure 2E). Synaptophysin LI was significantly lower in SUDEP than NEC for all ROI ($P < 0.05$ to $P < 0.01$) but no significant difference was observed between EPC and NEC (Figure 2F).
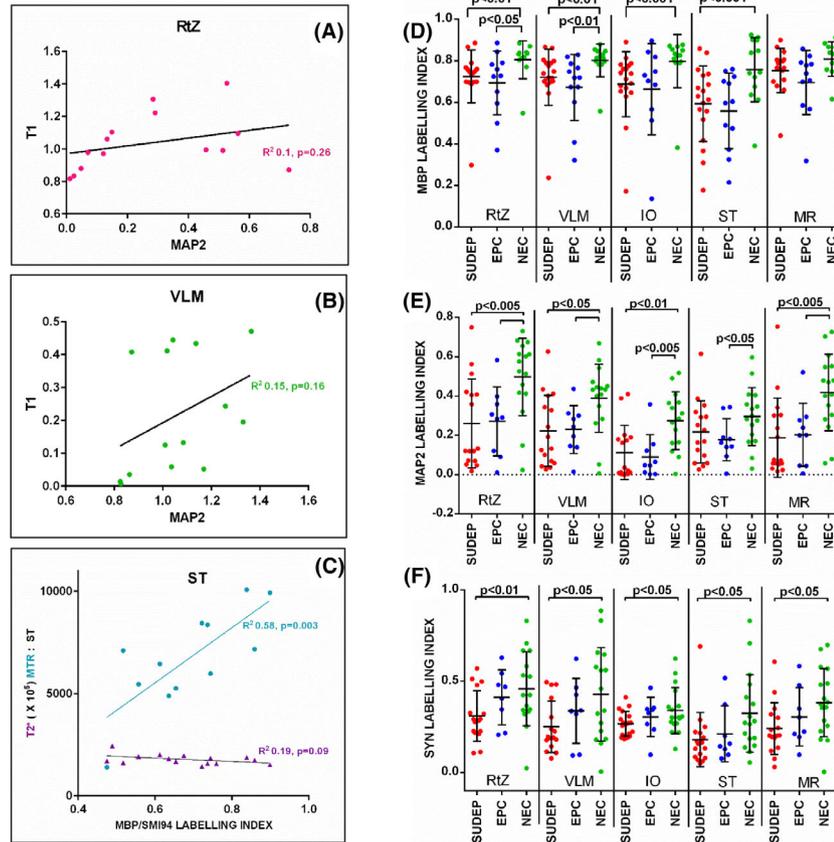
Figure 2. Quantitative MRI and pathology correlations and in cause of death groups. (**A**) In all 16 cases, there was a positive correlation between T1 values and MAP2 labelling index (LI) in the reticular zone (RtZ) ($P < 0.05$, Kendal's correlation test for nonparametric data with linear regression shown on graph) and (**B**) in the ventrolateral medulla (VLM) ($P < 0.05$, Kendal's correlation test for nonparametric data with linear regression shown on graph). (**C**) For myelin basic protein (MBP/SMI94) there was negative correlation with T2* in the solitary tract (ST) but a positive correlation with MTR ($P < 0.05$, Kendal's correlation test for nonparametric data with linear regression shown on graph). (**D**) In all 47 cases for all obex levels, scatter graphs of MBP LI in relation to regions of interest [RtZ, VLM, inferior olive (IO), ST and medullary raphe (MR)] in cause of death groups; mean SMI94/MBP LI was significantly lower in sudden unexpected death in epilepsy (SUDEP) and epilepsy controls (EPC) than in nonepilepsy controls (NEC) in the VLM and RtZ but there were no significant differences between SUDEP and EPC. (**E**) In all 47 cases for all obex levels, scatter graphs of MAP2 LI; mean LI was significantly lower in SUDEP and EPC groups than NEC for all region of interest (ROI) but there were no significant differences between EPC and SUDEP. (**F**) In all 47 cases for all obex levels, scatter graphs of synaptophysin (syn) LI; mean LI was significantly lower in SUDEP than NEC for all ROI but no significant difference was observed between EPC and NEC. Bars represent mean values in **D**–**F** and whiskers standard deviation.

Clinical and neuropathological factors There was no significant correlation between MRI or pathology measures and age at death. Age at seizure onset for the epilepsy group was not available in all cases (Table S1), so this was not further analysed. Epilepsy cases were categorized into pathology negative cases (no significant neuropathological abnormality) or with a confirmed lesional pathology at postmortem, for example hippocampal sclerosis, DNT, old scars, potentially relevant to cause or effect of seizures (see Table S1). There were no significant differences in

medullary volume estimates or SMI94/MBP, synaptophysin, MAP2 LI between cases with or without brain pathology. There were no significant differences in recorded brain weights between cause of death groups, but a positive correlation noted between Cavalieri-estimated AV of the RtZ and brain weight ($P < 0.05$).

Stratifying cases for obex levels The obex levels of the medullary samples that were available from the tissue bank archives were not identical between cases; in

many cases only a single medulla block was available. Although there was no significant difference in the mean mid-obex level between the cause of death groups (Table 1), the volume of the RtZ, as estimated by both MRI and Cavalieri methods were observed to increase with obex level (Figure S1C). We therefore stratified the 47 cases into three groups according to the mid-obex level of the block, for the Cavalieri volume estimation and for the neuropathological measures: caudal medulla <3 mm, mid-medulla 4–6 mm and rostral medulla >7 mm (Figure 3). Further analysis showed significantly greater actual RtZ volumes in the mid-medulla in the SUDEP group (but not EPC) compared to NEC (Figure 4A). In contrast, significantly lower RtZ RVs were noted in the rostral medulla in SUDEP compared to NEC ($P < 0.05$) (Figure 4B). For pathology measures significantly lower MAP2 were noted in rostral medulla ROI in epilepsy cases ($P < 0.03$ to $P < 0.004$) and lower MAP2 in the mid medulla in the RtZ in the SUDEP group alone compared to NEC ($P < 0.05$). SMI94 LI was significantly lower LI in the IO ROI only in epilepsy cases ($P < 0.05$) in the rostral medulla.

For the 16 cases with MRI, cases were stratified into two groups, caudal and rostral medulla (≤6 mm/ >6 mm). Significantly higher VLM volumes ($P < 0.05$) (Figures 3 and 4C) (and relative VLM volumes $P = 0.05$, (Figure 4D)) were noted in the caudal medulla in epilepsy cases but lower VLM volumes in the rostral medulla compared to NEC ($P < 0.05$) (Figure 4C). There was no statistical relationship between qMRI measurements and obex level or differences between cause of death groups when stratified into upper and lower medulla groups.

Postmortem variables The postmortem intervals (PMI) and fixation times (total time in formaldehyde prior to tissue processing) varied between cases as these were mainly coronial postmortem investigations carried out in different centres. Although not significantly different between the cause of death groups (Table 1) there was variability, with longer mean fixation times in EPCs but shorter PMI. For all 16 cases, a positive correlation between T1 and MTR values with PMI ($P < 0.05$) in the RtZ was noted but an inverse correlation between T1 values and fixation time ($P < 0.05$). Similar associations were also seen for the VLM and IO regions but not for T2/T2* values in any region. There were
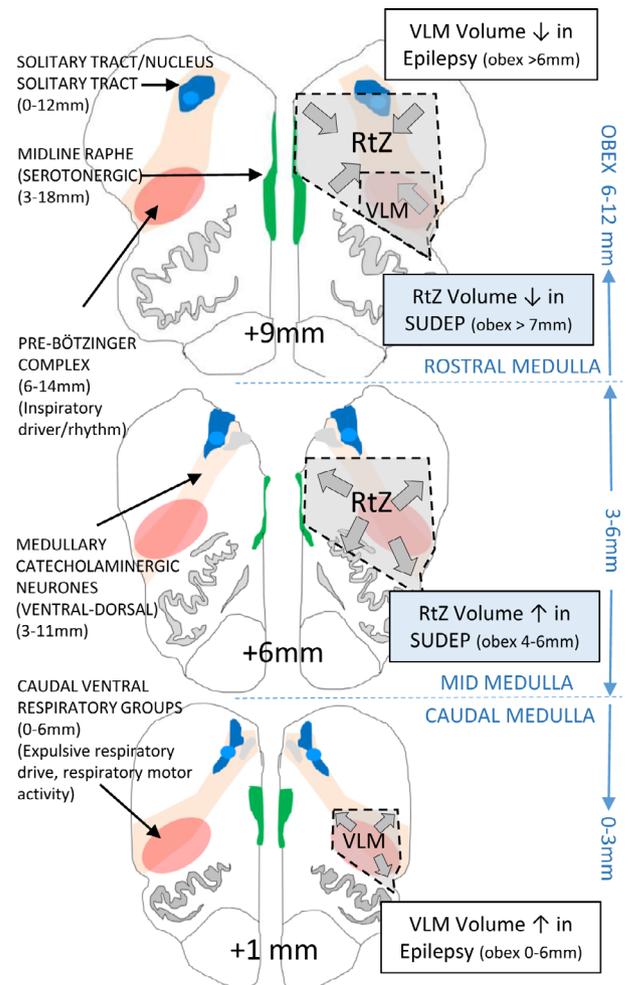
Figure 3. Diagrammatic representation of obex levels, respiratory autonomic nuclei and volume alterations in sudden unexpected death in epilepsy (SUDEP) and epilepsy. On the left hand side, the key respiratory nuclear regulatory groups are outlined and their approximate obex levels in the human medulla and position were indicated. On the right side, the volume changes noted in SUDEP and epilepsy cases were compared to controls when cases were grouped according to the obex level (rostral, mid or caudal). Volume contraction in the reticular zone (RtZ) of the rostral medulla and expansion in the caudal medulla was observed with the Cavalieri method in SUDEP cases (blue boxes) and similar volume changes in the ventrolateral medulla (VLM) region in epilepsy cases with MRI (white boxes).

no significant correlations between volume estimates (either on MRI or Cavalieri) or for SMI94/MBP LI with either PMI or fixation time. A negative correlation between fixation times and MAP2 LI ($P < 0.05$) and synaptophysin LI ($P < 0.005$) was noted.

Multivariate analysis We carried out multiple regression analysis to factor all independent variables
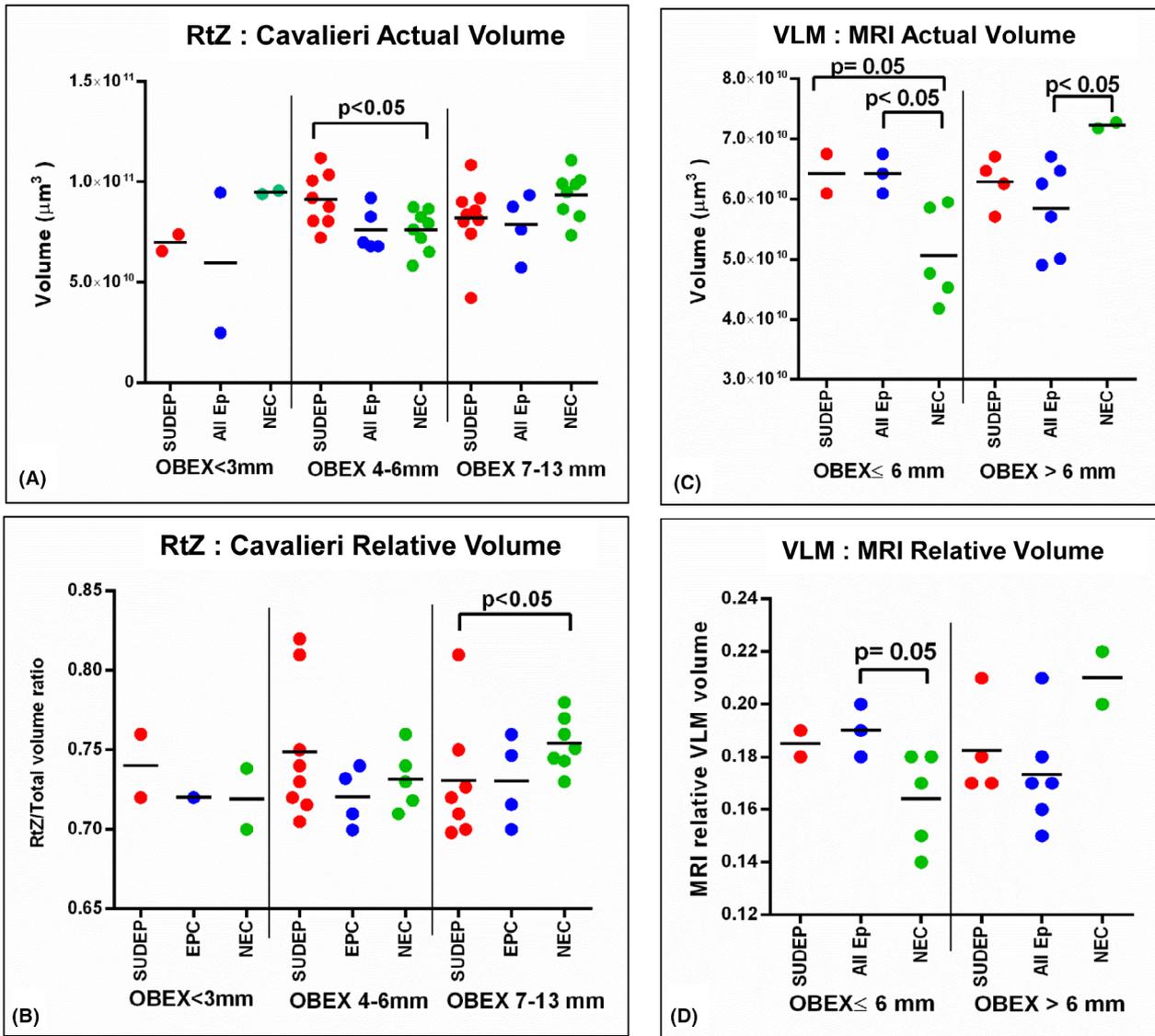
Figure 4. Variation of medulla volume estimations in reticular zone (RtZ) and ventrolateral medulla (VLM) between cause of death group stratified for obex levels. (**A**) Cavalieri volume estimates stratified into three groups, according to the mid-obex level (caudal medulla <3 mm, mid medulla 4–6 mm and rostral medulla >7 mm) showed significantly greater actual RtZ volumes in the mid-medulla regions in the sudden unexpected death in epilepsy (SUDEP) group compared to nonepilepsy controls (NEC). (**B**) Cavalieri relative volume estimates stratified into three groups, according to the mid-obex level (caudal medulla <3 mm, mid medulla 4–6 mm and rostral medulla >7 mm) showed significantly lower RtZ relative volumes in the rostral medulla in SUDEP compared to NEC. (**C**) Medullary volume estimates for the 16 cases with 9.4T MRI were stratified into two groups [caudal (≤6 mm) and rostral medulla (>6 mm)] and significantly higher actual VLM volumes were noted in the caudal medulla in epilepsy cases (All Ep) (and SUDEP group alone) but lower VLM volumes in the rostral medulla in all epilepsy cases compared to NEC (**D**) MRI relative VLM volumes also showed significant differences between epilepsy cases and NEC in the caudal medulla.

of fixation time, PMI and obex level effecting pathology and MRI measures. This further analysis confirmed no differences in qMRI values for any ROI between cause of death groups. MAP2 LI remained significantly lower in the rostral medulla RtZ in all epilepsy cases compared to NEC ($P < 0.05$).

Discussion

In this postmortem study, incorporating high resolution MRI of the brain stem, we provide further evidence for volume alterations in autonomic regulatory regions in SUDEP compared to controls, when aligning for the

obex level. We also observed differences in the level of medullary myelination and neuronal marker MAP2 in epilepsy cases compared to controls which could indicate brainstem neurodegeneration. Identification of alterations in the medulla in epilepsy will further the understanding of networks involved and pathways that could lead to SUDEP.

Volume change in medulla in SUDEP and epilepsy

Brain atrophy is accelerated in epilepsy. In the ENIGMA consortium of 2149 epilepsy patients, distinct patterns of reduced grey matter in cortical and subcortical structures were shown on MRI [25] and recent longitudinal MRI studies have confirmed progressive and accelerated regional cortical thinning in patients with focal epilepsy compared to control groups [26]. None of these studies looked into pathological correlations, but cortical neuronal loss or neurodegeneration is the proposed, unproven underlying process with regional patterns suggesting a selective vulnerability. The brainstem is rarely investigated in epilepsy but is relevant to SUDEP [27]. All MRI studies to date have used retrospective analysis of *in vivo* MRI investigations carried out at variable times prior to the SUDEP. In the report by Mueller *et al.*, based on *in vivo* 4T MRI, volume loss in the brainstem, including the upper medulla, was shown in one person who went on to have SUDEP compared to non-SUDEP controls [12]. This finding was supported in a subsequent study of 26 cases with 3T MRI, showing volume loss in autonomic ROI in the brainstem, including the midbrain periaqueductal grey, raphe nuclear regions and medulla in SUDEP [13]. Limitations due to the lower resolution reachable at 3T prevented delineation of anatomical brainstem structures but nevertheless their method ensured accurate rostro-caudal evaluation of volume loss [12]. A recent VBM study of 3T MRI from 25 SUDEP cases also showed volume loss in periaqueductal grey of the midbrain in addition to left thalamus, left hippocampus and posterior cingulate and cerebellum, but did not replicate findings in the medulla [11].

We did not observe differences in medulla regional volumes between the cause of death groups with either MRI or Cavalieri method for the whole cohort, but when stratifying cases according to their obex level, some significant rostro-caudal differences emerged. Decreased AVs specifically in the VLM region in the rostral medulla were seen in the epilepsy group on MRI and this was reinforced in our larger pathology series by decreased relative RtZ volumes in the rostral medulla and more specifically in the SUDEP group. The RtZ ROI includes both key medullary respiratory nuclear groups of the ventral respiratory column in the VLM, such as the pre-BötC, NA [24,25], as well as MR which contain serotonergic neurones with chemosensory regulatory properties [14]. In contrast, in the caudal medulla greater RtZ volumes were observed in the SUDEP group and greater actual and RVs in the VLM in all epilepsy cases on MRI. Knowledge of the connectivity of brainstem respiratory/autonomic networks is largely based on animals [14,15,28] as human fMRI studies lack the spatial resolution [29,30]. There is a hierarchical organization in a rostro-caudal direction of the ventral respiratory groups (VRG) in the VLM; the Bötzinger complex and pre-BötC, that control expiratory and inspiratory respiratory rhythms respectively, are more rostral than VRG that co-ordinate output to the phrenic and spinal motor neurones [14]. In the human brainstem, the pre-BötC is considered largest between obex levels 9–10 mm (Schwarzacher *et al.* [24]). Our observation of lower volumes in SUDEP cases in the rostral medulla could be relevant to pathology in the pre-BötC region. However, the higher RtZ volumes noted in SUDEP in the caudal medulla could implicate pathology in VRG that determines the motor control of respiration, of potential equal importance (Figure 3).

We also aimed to address the pathological correlation of MRI medullary volume changes in SUDEP. Quantitative *ex vivo* 9.4T MRI has the sensitivity to detect subtle differences in neuronal density, myelination and brainstem anatomy [31]. Indeed *in vivo* studies have demonstrated its utility to show microanatomical structures in the human midbrain [32]. In previous quantitative studies of epilepsy surgical samples with similar immunomarkers, a positive correlation between T1, T2* relaxation times and neuronal marker MAP2 but an inverse correlation with MTR was observed [23]. In contrast, myelin stains including SMI94/MBP show an inverse correlation with T1, T2, T2* but positive correlations with MTR in both cortex and white matter ROI [23,33]. In the current study, we noted similar correlations in many but not all ROI. This could partly be explained by the more complex intermingling of grey matter nuclei and white matter tracts in the medulla compared to their relative

compartmentalization in the neocortex. We did not, however, identify differences in these MRI quantitative values between the cause of death groups.

We noted reduced myelin content, based on MBP labelling, in the RtZ and VLM in epilepsy cases. There is evidence from both imaging and pathology studies of compromised myelination both in the vicinity and at distance from a focal epileptogenic focus, likely reflecting network changes due to seizures [34]. It is known that seizures can spread to the brain stem [35] and neuronal activity influences oligodendroglial proliferation, and myelin plasticity in epilepsy, although the pathological basis is not well-understood [36]. When we factored for obex level however, significantly reduced myelin labelling was only noted in the IO region in the SUDEP group. In contrast, neuronal and dendritic marker MAP2 was reduced in the rostral RtZ (>7 mm) in all epilepsy cases and the mid medulla (3–6 mm) in the SUDEP group only; following multivariate analysis, factoring fixation time effects, MAP2 LI remained significantly lower in the rostral medulla RtZ in epilepsy, but not specifically in the SUDEP group. Reduced MAP2 could indicate loss of neurones and/or dendritic branches or cellular MAP2 expression. There are mixed neuronal types in the RtZ including the pre-BötC, formed by interconnecting and modulating nuclei and networks [14] and characterized by multitransmitter systems [37]; these include pacemaker-like somatostatin/NK1R-positive cells of the pre-BotC and modulating serotonergic neurons in the MR and VLM. In a previous study we showed a reduction in somatostatin neuronal subsets in the VLM and tryptophan hydroxylase expressing serotonergic neurones in the VLM and MR, particularly in rostral medulla (obex 7–9 mm), the putative level of the pre-BötC in SUDEP [20]. In contrast, however, NK1R positive neurons in the VLM were predominantly reduced in the caudal medulla (3–4 mm) in SUDEP [20]. These rostro caudal variations reflect the differential MAP2 findings and volume alterations in the current series.

In a recent study addressing medullary glial populations, we did not identify any differences in overall GFAP astroglial labelling to suggest reactive gliosis in SUDEP, although diminished populations of specialized chemosensory glial subsets were identified [19]. We have also noted no significant reduction in medullary catecholaminergic neuronal populations in SUDEP (Patodia *et al.*, unpublished data) and in an earlier study we also reported no significant microglial activation in the medulla, hypoxic neuronal injury or loss of integrity of the blood brain barrier in SUDEP to suggest more acute medullary pathology [38]. Taken together these findings propose a chronic, regionally selective reduction in specific types of medullary neurones and glia, which collectively could explain the subtle quantitative volume alterations reported in the current and *in-vivo* MRI studies [12,13]. These alterations could be directly secondary to seizures or its effects. It is recognized that neuroplasticity in respiratory nuclei occurs, enabling a capacity for compensatory adaptation under physiological challenges [39] as well as disease states [14]. Chronic, intermittent hypoxia and hypercarbia result in augmentation of respiratory motor outputs [40], likely involving serotonergic networks, their connections to the preBötC [41] and central chemoreception [42]. For example, a recent experimental study demonstrated a reduction in the number of serotonergic and total NeuN-positive neurons in the MR and VLM following 30 days of increased CO_2 [43]. It is plausible that recurrent generalized seizures with associated, albeit intermittent, episodes of hypoxia and hypercarbia induce respiratory plasticity in brainstem nuclei which could influence vulnerability to SUDEP. Further work to understand brainstem networks in epilepsy and SUDEP is clearly needed.

Limitations include that as an archival study, different levels of the medulla had been sampled and fixation times varied between cases which we have factored in the analysis. Our SUDEP group included both definite and possible/probable cases according to current criteria [22]; however, there were no differences in the pathology and volume measurements between these SUDEP groups (data not shown). *Ex-vivo* MRI methods were based on a small sample size of 16 and MTR values only achieved on one EPC. Furthermore, *in-vivo* MRI volume analysis, such as voxel-based morphometry, include steps where whole brains are spatially 'normalized' to a template to account for individual differences in brain shape. Such a step is not available for this *ex-vivo* study. We calculated RVs in addition to AV estimates of the RtZ in an aim to address case differences, tissue processing effects and nonaxial section planes. We also identified higher IO volumes in all epilepsy cases as an unexplained finding on MRI and we

cannot exclude that this has influenced the RV estimates. In addition, the co-registration between MRI and pathology slices was carried out by manual alignment and we have only examined a 2 mm axial length of the medulla from each case in the relatively small number that had 9.4T MRI. Further studies of brainstem regional volumes, including the pons and midbrain, are essential to evaluate any global brainstem alterations in epilepsy and SUDEP.

In summary, our study findings suggest a rostro-caudal alteration in medullary volume and neuronal composition in the RtZ in epilepsy and SUDEP. As these localize with regions containing respiratory regulatory nuclei, they could represent seizure-related alterations, as a SUDEP vulnerability factor and potential disease biomarker.

Acknowledgements

Ethical approval

Tissue from all cases was retained with era-appropriate consent and the project has ethical approval (through NRES 17/SC/0573).

Author contributions

SP, AS: Conducting the laboratory investigations including sample preparations and image analysis; MTa, XG, TY: MRI analysis of samples; SS, IS: Clinical neurology data; MTh, SP: data analysis and manuscript preparation; SP, MTh, XG, TY, MT: study design; All authors: Manuscript review.

Conflict of interest

The authors in this article have no conflicts of interest to disclose. The Editors of Neuropathology and Applied Neurobiology are committed to peer-review integrity and upholding the highest standards of review. As such, this article was peer-reviewed by independent, anonymous expert referees and the corresponding author had no role in either the editorial decision or the handling of the paper.

Data availability statement

The data that support the findings of this study are available from the corresponding author upon reasonable request.

References

1 Devinsky O, Hesdorffer DC, Thurman DJ, Lhatoo S, Richerson G. Sudden unexpected death in epilepsy: epidemiology, mechanisms, and prevention. *Lancet Neurol* 2016; **15**: 1075–88

2 Ryvlin P, Nashef L, Lhatoo SD, Bateman LM, Bird J, Bleasel A, et al. Incidence and mechanisms of cardiorespiratory arrests in epilepsy monitoring units (MORTEMUS): a retrospective study. *Lancet Neurol* 2013; **12**: 966–77

3 Harden C, Tomson T, Gloss D, Buchhalter J, Cross JH, Donner E, et al. Practice guideline summary: sudden unexpected death in epilepsy incidence rates and risk factors: report of the guideline development, dissemination, and implementation subcommittee of the American Academy of Neurology and the American Epilepsy Society. *Neurology* 2017; **88**: 1674–80

4 DeGiorgio CM, Markovic D, Mazumder R, Moseley BD. Ranking the leading risk factors for sudden unexpected death in epilepsy. *Front Neurol* 2017; **8**: 473

5 Simon RP. Heart and lung in the postictal state. *Epilepsy Behav* 2010; **19**: 167–71

6 Lacuey N, Zonjy B, Hampson JP, Rani MRS, Zaremba A, Sainju RK, et al. The incidence and significance of

periictal apnea in epileptic seizures. *Epilepsia* 2018; **59**: 573–82

7 Vilella L, Lacuey N, Hampson JP, Rani MRS, Sainju RK, Friedman D, et al. Postconvulsive central apnea as a biomarker for sudden unexpected death in epilepsy (SUDEP). *Neurology* 2019; **92**: e171–e182

8 Bruno E, Maira G, Biondi A, Richardson MP. Ictal hypoxemia: a systematic review and meta-analysis. *Seizure* 2018; **63**: 7–13

9 Sveinsson O, Andersson T, Carlsson S, Tomson T. Circumstances of SUDEP: a nationwide population-based case series. *Epilepsia* 2018; **59**: 1074–82

10 Aiba I, Noebels JL. Spreading depolarization in the brainstem mediates sudden cardiorespiratory arrest in mouse SUDEP models. *Sci Transl Med* 2015; **7**: 282ra46

11 Allen LA, Vos SB, Kumar R, Ogren JA, Harper RK, Winston GP, et al. Cerebellar, limbic, and midbrain volume alterations in sudden unexpected death in epilepsy. *Epilepsia* 2019; **60**: 718–29

12 Mueller SG, Bateman LM, Laxer KD. Evidence for brainstem network disruption in temporal lobe epilepsy and sudden unexplained death in epilepsy. *Neuroimage Clin* 2014; **5**: 208–16

13 Mueller SG, Nei M, Bateman LM, Knowlton R, Laxer KD, Friedman D, et al. Brainstem network disruption: a pathway to sudden unexplained death in epilepsy? *Hum Brain Mapp* 2018; **39**: 4820–4830

14 Smith JC, Abdala AP, Borgmann A, Rybak IA, Paton JF. Brainstem respiratory networks: building blocks and microcircuits. *Trends Neurosci* 2013; **36**: 152–62

15 Koshiya N, Oku Y, Yokota S, Oyamada Y, Yasui Y, Okada Y. Anatomical and functional pathways of rhythmogenic inspiratory premotor information flow originating in the pre-Botzinger complex in the rat medulla. *Neuroscience* 2014; **268**: 194–211

16 Ramirez-Jarquin JO, Lara-Hernandez S, Lopez-Guerrero JJ, Aguileta MA, Rivera-Angulo AJ, Sampieri A, et al. Somatostatin modulates generation of inspiratory rhythms and determines asphyxia survival. *Peptides* 2012; **34**: 360–72

17 Wei XY, Zhao Y, Wong-Riley MT, Ju G, Liu YY. Synaptic relationship between somatostatin- and neurokinin-1 receptor-immunoreactive neurons in the pre-Botzinger complex of rats. *J Neurochem* 2012; **122**: 923–33

18 Benarroch EE. Medullary serotonergic system: organization, effects, and clinical correlations. *Neurology* 2014; **83**: 1104–11

19 Patodia S, Paradiso B, Ellis M, Somani A, Sisodiya SM, Devinsky O, et al. Characterisation of medullary astrocytic populations in respiratory nuclei and alterations in sudden unexpected death in epilepsy. *Epilepsy Res* 2019; **157**: 106213

20 Patodia S, Somani A, O'Hare M, Venkateswaran R, Liu J, Michalak Z, et al. The ventrolateral medulla and medullary raphe in sudden unexpected death in epilepsy. *Brain* 2018; **141**: 1719–33

21 Catarino CB, Liu JY, Liagkouras I, Gibbons VS, Labrum RW, Ellis R, et al. Dravet syndrome as epileptic encephalopathy: evidence from long-term course and neuropathology. *Brain* 2011; **134**(Pt 10): 2982–3010

22 Nashef L, So EL, Ryvlin P, Tomson T. Unifying the definitions of sudden unexpected death in epilepsy. *Epilepsia* 2012; **53**: 227–33

23 Reeves C, Tachrount M, Thomas D, Michalak Z, Liu J, Ellis M, et al. Combined ex vivo 9.4T MRI and quantitative histopathological study in normal and pathological neocortical resections in focal epilepsy. *Brain Pathol* 2016; **26**: 319–33

24 Schwarzacher SW, Rub U, Deller T. Neuroanatomical characteristics of the human pre-Botzinger complex and its involvement in neurodegenerative brainstem diseases. *Brain* 2011; **134**(Pt 1): 24–35

25 Paxinos G, Huang XF. *Atlas of the Human Brainstem*. San Diego: Academic Press, 1995.

26 Whelan CD, Altmann A, Botia JA, Jahanshad N, Hibar DP, Absil J, et al. Structural brain abnormalities in the common epilepsies assessed in a worldwide ENIGMA study. *Brain* 2018; **141**: 391–408

27 Galovic M, van Dooren VQH, Postma T, Vos SB, Caciagli L, Borzi G, et al. Progressive cortical thinning in patients with focal epilepsy. *JAMA Neurol* 2019; **76**: 1230

28 Englot DJ, Gonzalez HFJ, Reynolds BB, Konrad PE, Jacobs ML, Gore JC, et al. Relating structural and functional brainstem connectivity to disease measures in epilepsy. *Neurology* 2018; **91**(1): e67–e77

29 Ikeda K, Kawakami K, Onimaru H, Okada Y, Yokota S, Koshiya N, et al. The respiratory control mechanisms in the brainstem and spinal cord: integrative views of the neuroanatomy and neurophysiology. *J Physiol Sci* 2017; **67**: 45–62

30 Pattinson KT, Mitsis GD, Harvey AK, Jbabdi S, Dirckx S, Mayhew SD, et al. Determination of the human brainstem respiratory control network and its cortical connections in vivo using functional and structural imaging. *NeuroImage* 2009; **44**: 295–305

31 Feldman JL, Del Negro CA. Looking for inspiration: new perspectives on respiratory rhythm. *Nat Rev Neurosci* 2006; **7**: 232–42

32 Massey LA, Miranda MA, Al-Helli O, Parkes HG, Thornton JS, So PW, et al. 9.4T MR microscopy of the substantia nigra with pathological validation in controls and disease. *Neuroimage Clin* 2017; **13**: 154–63

33 Loureiro JR, Himmelbach M, Ethofer T, Pohmann R, Martin P, Bause J, et al. In-vivo quantitative structural imaging of the human midbrain and the superior colliculus at 9.4T. *NeuroImage* 2018; **177**: 117–28

34 Garbelli R, Zucca I, Milesi G, Mastropietro A, D'Incerti L, Tassi L, et al. Combined 7-T MRI and

histopathologic study of normal and dysplastic samples from patients with TLE. *Neurology* 2011; **76**: 1177–85

35 Deleo F, Thom M, Concha L, Bernasconi A, Bernhardt BC, Bernasconi N. Histological and MRI markers of white matter damage in focal epilepsy. *Epilepsy Res* 2018; **140**: 29–38

36 Cavanna AE, Monaco F. Brain mechanisms of altered conscious states during epileptic seizures. *Nat Rev Neurol* 2009; **5**: 267–76

37 Gibson EM, Geraghty AC, Monje M. Bad wrap: myelin and myelin plasticity in health and disease. *Dev Neurobiol.* 2018; **78**: 123–35

38 Ramirez JM, Doi A, Garcia AJ 3rd, Elsen FP, Koch H, Wei AD. The cellular building blocks of breathing. *Compr Physiol* 2012; **2**: 2683–731

39 Michalak Z, Obari D, Ellis M, Thom M, Sisodiya SM. Neuropathology of SUDEP: role of inflammation, blood-brain barrier impairment, and hypoxia. *Neurology* 2017; **88**: 551–61

40 Doi A, Ramirez JM. State-dependent interactions between excitatory neuromodulators in the neuronal control of breathing. *J Neurosci* 2010; **30**: 8251–62

41 Mitchell GS, Baker TL, Nanda SA, Fuller DD, Zabka AG, Hodgeman BA, et al. Invited review: Intermittent hypoxia and respiratory plasticity. *J Appl Physiol* 2001; **90**: 2466–75

42 Kang JJ, Liang WH, Lam CS, Huang XF, Yang SJ, Wong-Riley MT, et al. Catecholaminergic neurons in synaptic connections with pre-Botzinger complex neurons in the rostral ventrolateral medulla in normoxic and daily acute intermittent hypoxic rats. *Exp Neurol* 2017; **287**(Pt 2): 165–75

43 Reeves SR, Guo SZ, Brittian KR, Row BW, Gozal D. Anatomical changes in selected cardio-respiratory brainstem nuclei following early post-natal chronic intermittent hypoxia. *Neurosci Lett* 2006; **402**: 233–7

44 Burgraff NJ, Neumueller SE, Buchholz KJ, LeClaire J, Hodges MR, Pan L, et al. Brainstem serotonergic, catecholaminergic, and inflammatory adaptations during chronic hypercapnia in goats. *FASEB J* 2019; **33**: 14491–505

Supporting information

Additional Supporting Information may be found in the online version of this article at the publisher's web-site:

Figure S1. Alignment of MRI and cresyl-violet sections shown for hemi-brainstems and increased volume estimates of the reticular zone (RtZ) with higher obex level. (**A/A′**) T2 weighted image and aligned cresyl violet section of hemi-brainstem from case 22 (nonepilepsy control), obex range 4–6 mm and **B/B′** from case 1 (sudden unexpected death in epilepsy), obex range 8–10 mm. (**C**) Variations of volume estimates of the RtZ with obex levels through the medulla (mean and standard deviations shown). Higher volumes were obtained on MRI than on tissue sections, which partly results from tissue processing effects and shrinkage, but there was an overall correlation between the volume measurements with the two methods.

Table S1. Details of the cause of death, clinical details and main pathology findings in 47 cases.